Science Signaling

Supplementary Materials for

14-3-3 binding creates a memory of kinase action by stabilizing the modified state of phospholamban

Julia Menzel, Daniel Kownatzki-Danger, Sergiy Tokar, Alice Ballone, Kirsten Unthan-Fechner, Markus Kilisch, Christof Lenz, Henning Urlaub, Mattia Mori, Christian Ottmann, Michael J. Shattock, Stephan E. Lehnart, Blanche Schwappach*

*Corresponding author. Email: blanche.schwappach@med.uni-goettingen.de

The PDF file includes:

Other Supplementary Material for this manuscript includes the following:

(available at stke.sciencemag.org/cgi/content/full/13/647/eaaz1436/DC1)
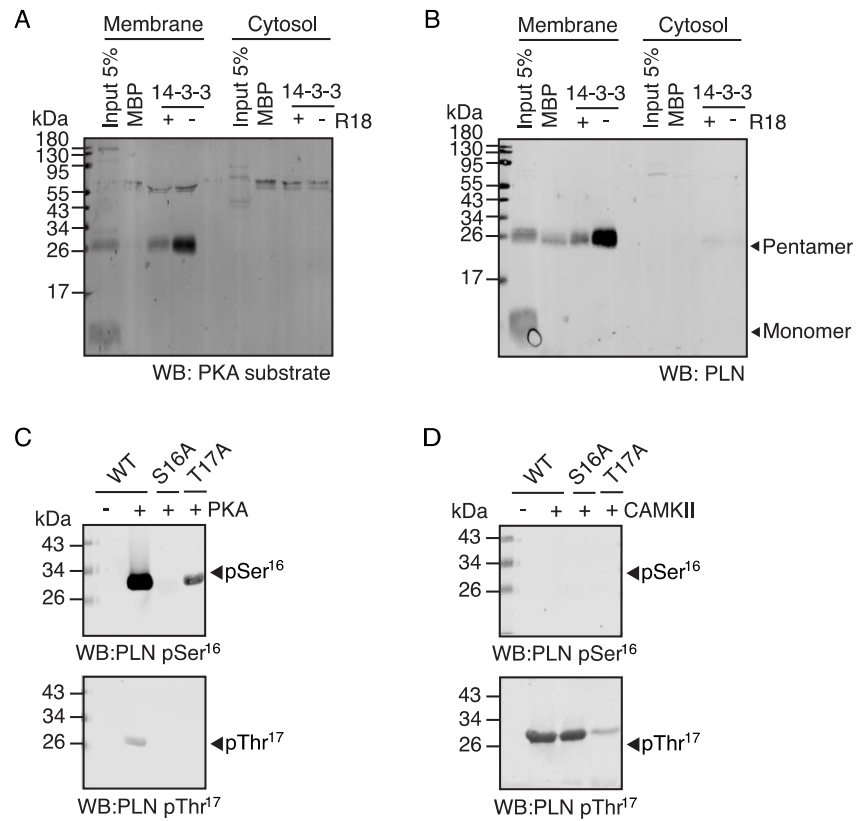
Fig. S1. Cardiac cytosolic fractions do not show a signal for 14-3-3–bound PLN. (**A**) Presence of PKA-phosphorylated proteins in the 14-3-3-bound membrane fraction but not in the cytosolic fraction (n = 3 mice/group). (**B**) Detection of 14-3-3-bound proteins from membrane or cytosolic fractions from cardiomyocytes with a PLN antibody (n = 6 mice/group). (**C,D**) Recombinant PLN WT, S16A, or T17A proteins were phosphorylated with either PKA (C) or CaMKII (D). The phosphorylated samples were resolved by SDS-PAGE and probed with pSer^{16}-PLN or pThr^{17}-PLN antibodies (n = 2 independent experiments). R18, R18 trifluoroacetate; WB, Western blot.

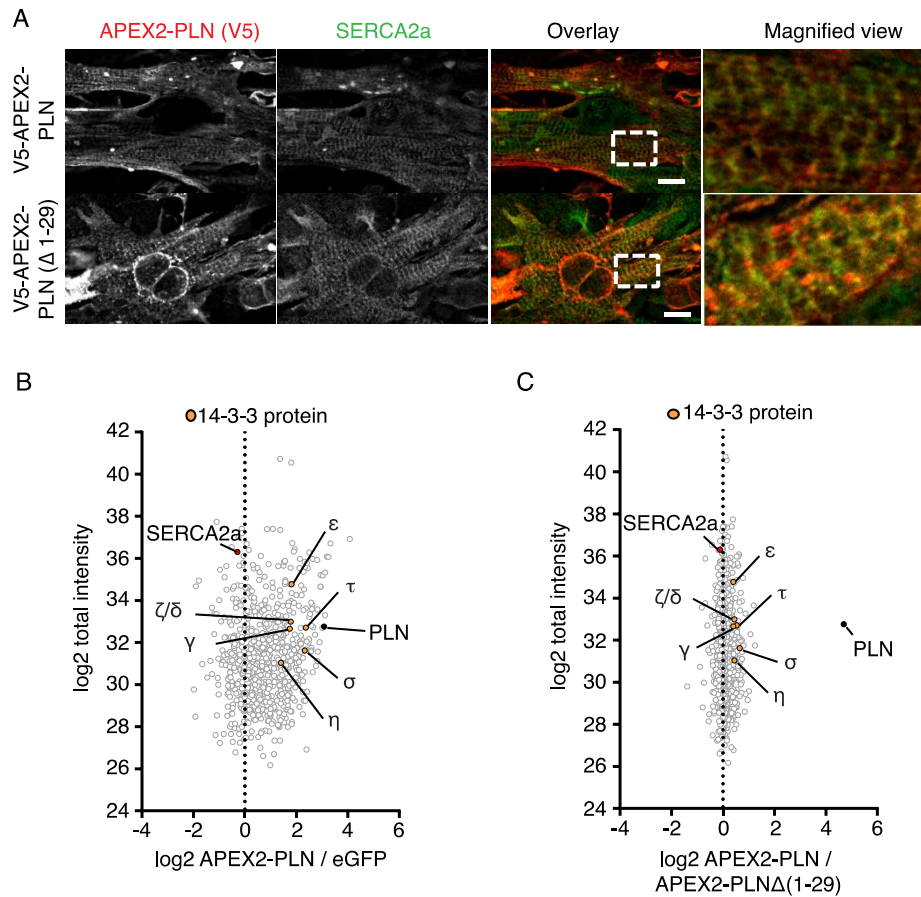**Fig. S2. Confocal imaging showing the colocalization of APEX2-PLN or APEX2-PLN (Δ1–29) and SERCA2a in NRCMs.** (**A**) NRCMs cultured for 15 days were transduced with adenoviruses (Ad5) expressing either APEX2-PLN or APEX2-PLN(Δ1-29). NRCMs were fixed with 4% paraformaldehyde, immunostained for V5 (red) and SERCA2a (green), and imaged by confocal microscopy (Zeiss LSM 880, 63x/1.4 Oil DIC objective). Dashed boxes indicate areas of magnified views (representative of 2 independent experiments). Scale bars 10 μm. (**B, C**) Log(2) dot plots showing all detected proteins for the ratio V5-APEX2-PLN/eGFP (B) or V5-APEX2-PLNΔ(1-29)/eGFP (C) (n=5 independent experiments from 3 NRCM preparations). δ, 14-3-3 delta; η, 14-3-3 eta; ε, 14-3-3 epsilon; γ, 14-3-3 gamma; σ, 14-3-3 sigma; τ, 14-3-3 tau; ζ, 14-3-3 zeta.

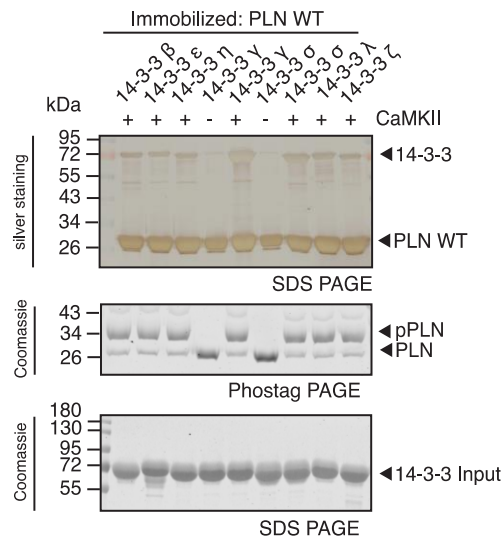**Fig. S3. All seven 14-3-3 isoforms bind pThr^{17}-PLN-GST.** Detection of PLN bound 14-3-3 isoforms with silver stained SDS PAGE. Unphosphorylated PLN-GST was used as negative control for the binding of 14-3-3γ and 14-3-3σ. Equal 14-3-3 inputs were confirmed on SDS PAGE and PLN pThr^{17} phosphorylation using activated CaMKII kinase was confirmed on a phostag gel (n = 3 independent experiments).
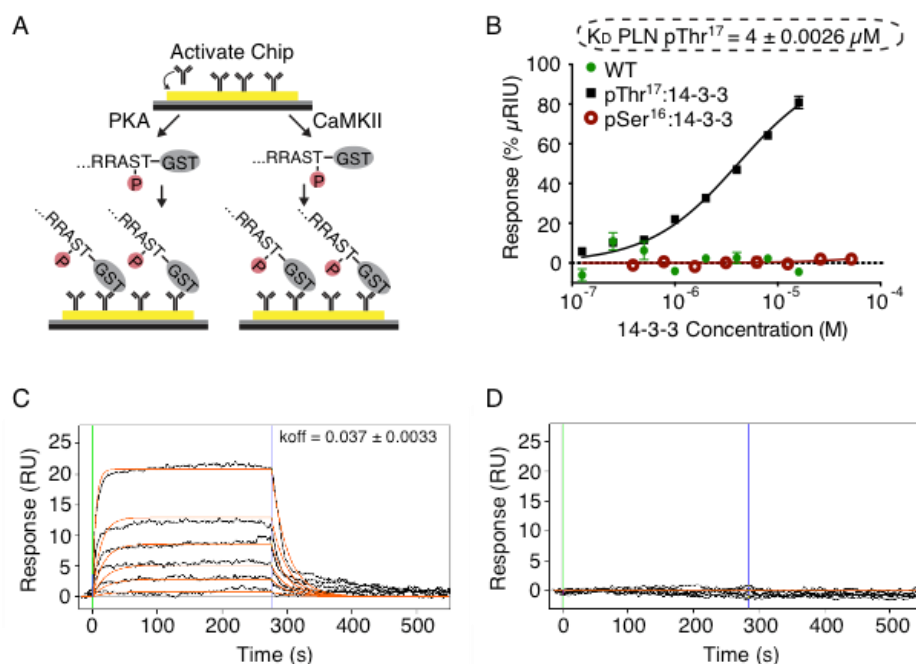
Fig. S4. Determination of the equilibrium dissociation constant for 14-3-3 binding to pThr[17]-PLN. (**A**) Scheme of surface plasmon resonance experiment using pSer[16]- or pThr[17]-PLN-GST. (**B**) Binding isotherm obtained from the experiment schematized in (A) and dissociation constant for 14-3-3γ (without MBP tag) binding pThr[17]-PLN determined by a sigmoidal dose-response curve fit (n = 3 independent experiments). Error bars depict +/-SEM. (**C, D**) Sensograms underlying (B) for pThr[17]-PLN (C) and unphosphorylated PLN exposed to the same concentrations of 14-3-3γ (D). K_D, equilibrium dissociation constant; pSer[16], PLN phosphorylated at Ser[16]; pThr[17], PLN phosphorylated at Thr[17]; koff, dissociation rate constant.

Fig. S5. MD simulation of the 14-3-3σ–pSer[16]–PLN complex and the 14-3-3σ–pThr[17]–PLN complex. (**A**) RMSD of all-atom of 14-3-3σ pr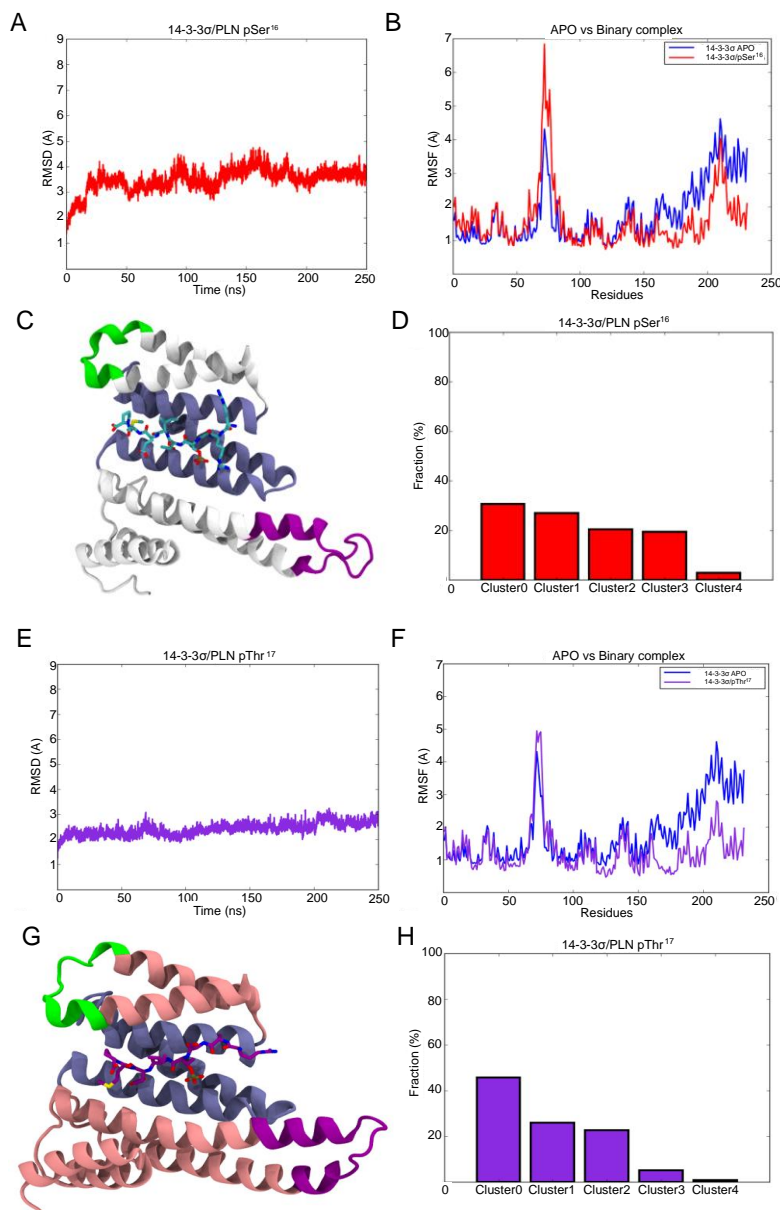otein and the peptide as a function of the MD simulation time. (**B**) RMSF of the protein residues of 14-3-3σ/pSer[16]-PLN complex (red curve) in comparison with 14-3-3σ apo (blue curve) obtained during the 250 ns simulation (n= 2 independent experiments). (**C**) Overview of 14-3-3σ monomer bound to pSer[16]-PLN (cyan sticks). Residues showing high conformational freedom in MD simulation are depicted in purple and green (loops 64-88 and 208-219, respectively). Residues 118-190 of the amphipathic groove are highlighted in ice blue. (**D**) Conformations of the 14-3-3σ-pSer[16]-PLN complex were clustered along MD trajectory frames. (**E**) RMSD of all-atom of 14-3-3σ protein and the peptide as a function of the MD simulation time. (**F**) RMSF of the protein residues of 14-3-3σ/pThr[17]-PLN complex (violet curve) in comparison with 14-3-3σ apo (blue curve) obtained during the 250 ns simulation (n = 2 independent experiments). (**G**) Overview of 14-3-3σ monomer bound to pThr[17]-PLN (purple sticks). Residues unfavourable for stability

during the simulation are depicted in purple and green. The amphipathic groove is highlighted in ice blue. (**H**) Conformations of the 14-3-3σ-pThr[17]-PLN complex were clustered along MD trajectory frames. 14-3-3σ, 14-3-3 sigma; RMSD, all-atom root mean square deviations; RMSF, root mean square fluctuation.

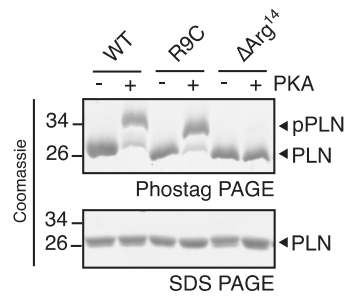**Fig. S6. PKA does not phosphorylate ΔArg¹⁴-PLN monomers.** In vitro phosphorylation of the indicated PLN variants using PKA (n = 3 independent experiments), visualized on phostag gel or SDS PAGE gel. pPLN, phosphorylated PLN.
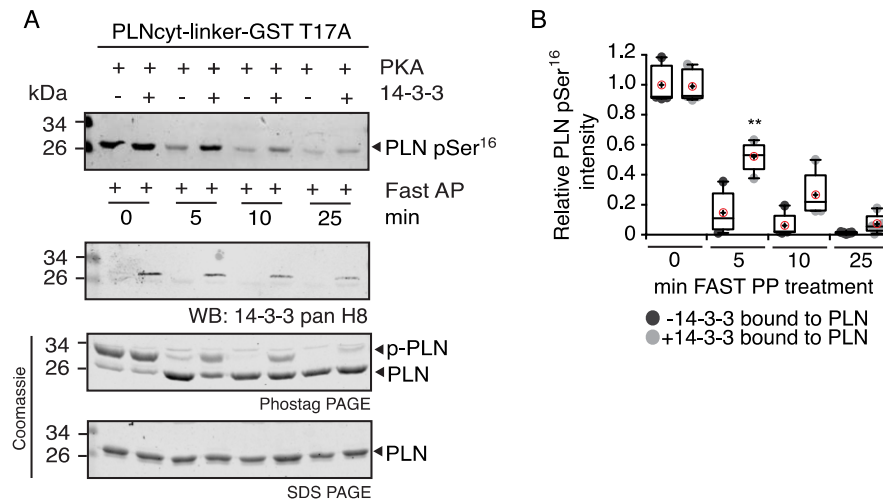
Fig. S7. 14-3-3 binding protects pSer[16]-T17A-PLN from fast dephosphorylation. (**A**) Dephosphorylation of pSer[16]-PLN T17A-GST in the presence of 14-3-3 was analysed by Western blot with anti-pSer[16]-PLN and 14-3-3 pan H8 antibodies (n = 5 independent experiments). In addition, pSer[16]-PLN was monitored on phos-tag gel and SDS PAGE gel. (**B**) Quantification of slower-migrating band observed in Phostag PAGE normalized to slower-migrating band at time point 0 (no 14-3-3) shown in (A). Data is presented as box and whisker plot with mean and median. A paired t-test showed no significant difference between the samples with or without 14-3-3 at 0 min (p=0.4279), at 10 min (p=0.0540) or at 25 min (p=0.0947). A significant difference was observed at 5 min (** p=0.0061). FastAP, alkaline phosphatase; min, minutes; pPLN, phosphorylated PLN.

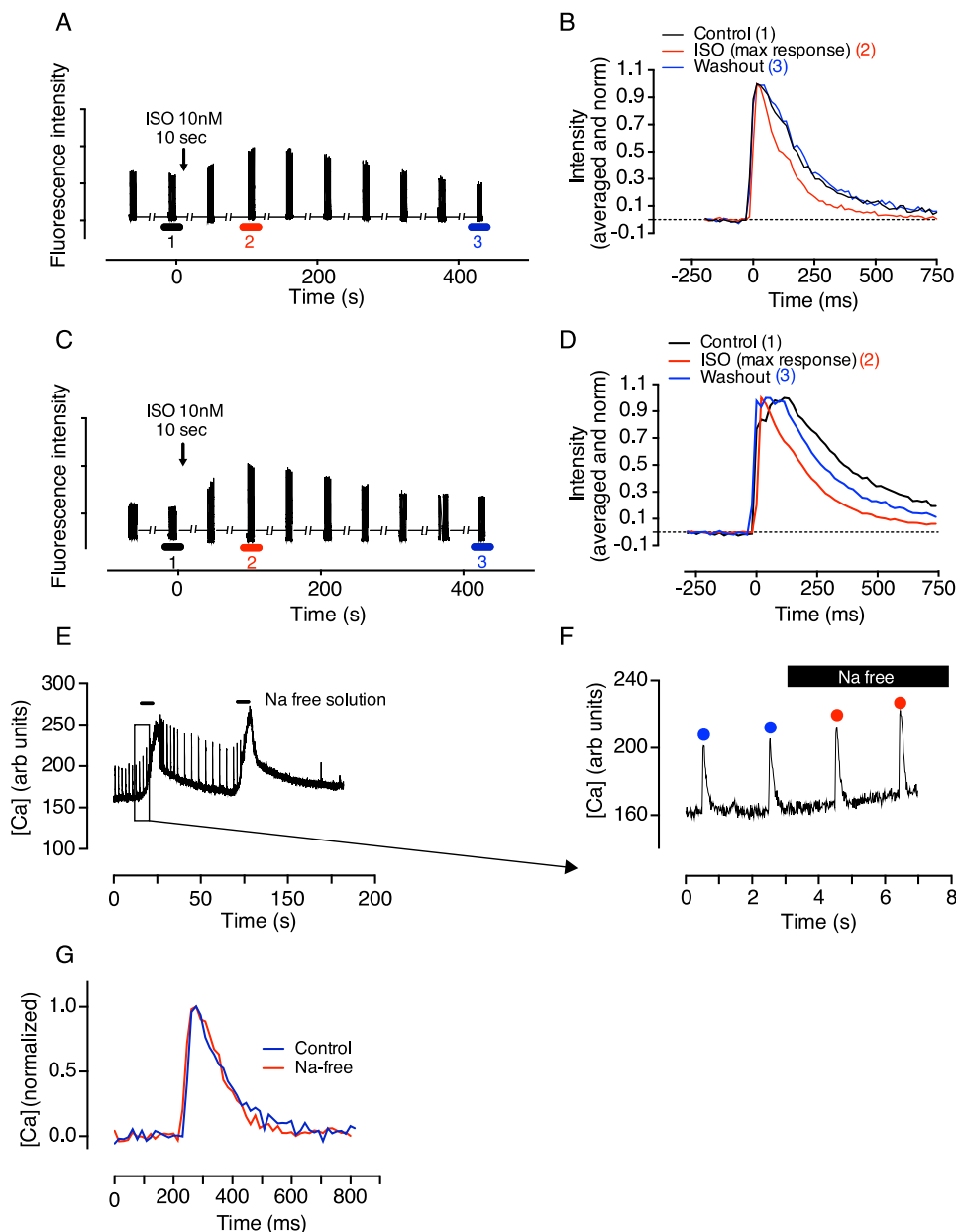**Fig. S8. Effect of 14-3-3 and Na⁺-free superfusion on the kinetics of isoprenaline-induced Ca²⁺ transients in isolated cardiomyocytes.** (**A**) Ca²⁺ transients were stimulated at 0.5 Hz by patch pipette and Ca²⁺ transients recorded discontinuously (due to memory buffering limitations of the video capture system). A 10 sec pulse of isoprenaline (ISO, 10 nM) was applied at the time point indicated. Representative traces from 7 myocytes isolated from 4 mice recorded with control pipette solution. (**B**) Ca²⁺ transient profiles averaged from 5 consecutive Ca²⁺ transients recorded at the points marked 1, 2 and 3 in (A). Data were normalized to maximum amplitude before plotting. (**C**) Ca²⁺ transients recorded as in (A) with a pipette solution containing 2µM of 14-3-3 in the whole-cell configuration. Representative of 7 myocytes isolated from 5 mice. (**D**) Ca²⁺ transient profiles averaged from 5 consecutive Ca²⁺ transients recorded with 14-3-3 in the pipette at the points marked 1, 2 and 3 in (C). Data were normalized to maximum amplitude before plotting. (**E**) Myocytes were stimulated throughout at 0.5 Hz by patch pipette and Ca²⁺ transients recorded. At the time points indicated, extracellular Na⁺ was rapidly and transiently replaced with an equimolar amount of mannitol. Representative of 5 myocytes isolated from 2 mice. (**F**) Magnified

section of (E) showing Ca^{2+} transient profiles immediately before and during perfusion with the Na^+-free solution. Representative of 5 myocytes isolated from 2 mice. (**G**) The final two Ca^{2+} transients in normal Tyrode (blue) and the first two transients in Na^+-free (red) were baseline corrected, normalized and averaged. Because Na^+-free perfusion inevitably loads the cell with Ca and causes an inotropy and diastolic shortening from which the cell ultimately does not recover. For this reason, only the first two Na^+-free transients were analyzed. Similar results were observed in 4 other cells.

Table S1. Plasmids used in this study.

Plasmid name	Description	Restriction sites inserted at	Source
pMal2CX	Bacterial expression vector for N-terminal MBP-tagged proteins	EcoRI - HindIII	New England BioLabs
pMal2CX 14-3-3β	Bacterial expression vector for MBP-14-3-3β	EcoRI - HindIII	M. Kilisch
pMal2CX 14-3-3ε	Bacterial expression vector for MBP-14-3-3ε	EcoRI - HindIII	M. Kilisch
pMal2CX 14-3-3η	Bacterial expression vector for MBP-14-3-3η	EcoRI - HindIII	M. Kilisch
pMal2CX 14-3-3γ	Bacterial expression vector for MBP-14-3-3γ	EcoRI - HindIII	J.Menzel
pMal2CX 14-3-3σ	Bacterial expression vector for MBP-14-3-3σ	EcoRI - HindIII	M. Kilisch
pMal2CX 14-3-3τ	Bacterial expression vector for MBP-14-3-3τ	EcoRI - HindIII	M. Kilisch
pMal2CX 14-3-3ζ	Bacterial expression vector for MBP-14-3-3ζ	EcoRI - HindIII	M. Kilisch
pMal2CX - GST modified	Bacterial expression for C-terminal tagged GST proteins (MBP tag removed)	NdeI - BamHI	J. Menzel
pMal2CX modified PLN N31 WT	Bacterial expression vector for PLNcyt-linker-GST N31 WT	NdeI-XhoI	J. Menzel
pMal2CX modified PLN N31 S16A	Bacterial expression vector for PLNcyt-linker-GST N31 S16A	NdeI-XhoI	J. Menzel
pMal2CX modified PLN N31 T17A	Bacterial expression vector for PLNcyt-linker-GST N31 T17A	NdeI-XhoI	J. Menzel
pMal2CX modified PLN N31 S10A	Bacterial expression vector for PLNcyt-linker-GST N31 S10A	NdeI-XhoI	J. Menzel
pMal2CX modified PLN N31 R9C	Bacterial expression vector for PLNcyt-linker-GST N31 R9C	NdeI-XhoI	J. Menzel
pMal2CX modified PLN N31 R9A	Bacterial expression vector for PLNcyt-linker-GST N31 R9A	NdeI-XhoI	J. Menzel
pMal2CX modified PLN N31 ΔArg14	Bacterial expression vector for PLNcyt-linker-GST N31 R14del	NdeI-XhoI	J. Menzel

Table S2. Antibodies used in this study.

Name	Raised in	Supplier	Cat. No.	Dilution	Technique	PID*
14-3-3 pan (H8)	mouse	Santa Cruz	sc-1657	1:1000	Western	16
14-3-3 pan	rabbit	Abcam	ab14112	1:1000	Western	974
GST	rabbit	Carl Roth	3998.1	200 nM	SPR	66
Na/K ATPase α	mouse	Santa Cruz	sc-21712	1:1000	Western	20
p-PKA substrate	rabbit	Cell Signaling	9624	1:500	Western	522
PLN	mouse	Abcam	ab2865	1:1000	Western	520
PLN	rabbit	Lehnart lab	-	5 µl	IP	-
PLN pSer[16]	rabbit	Badrilla	A010-12	1:1000	Western	519
PLN pThr[17]	rabbit	Badrilla	A010-13	1:1000	Western	975
SERCA2a	rabbit	Badrilla	A010-20	1:200	IF	976
V5	mouse	Invitrogen	R960-25	1:200	IF	977

*persistent identifier generated by ePIC (https://www.pidconsortium.net)
https://hdl.handle.net/11022/umg-sfb1002-antibody-primary-XXX

Data file S1. In vivo proximity labeling. List of biotinylated proteins detected with a significance of $p < 0.01$ by in vivo proximity labeling using V5-APEX2-PLN.